A NEW VERSION OF THE LWR FUEL PERFORMANCE MODEL WAFER

NIELS KJAER-PEDERSEN

*Elsinore Shipbuilding and Engineering Company**

SUMMARY

Introduction. — This contribution discusses the latest version, WAFER-2, of the Danish LWR fuel performance code WAFER. The original version, WAFER-1, has previously been published.

Modifications in the new version are:

(i) Restrictions on fuel crack penetration have been completely removed. This implies more accurate stress analysis, hence more realistic creep calculations.

(ii) Several transversal fuel cracks at arbitrary axial locations (as opposed to one at the mid-pellet position in WAFER-1) are now permitted. This further improves stress analysis and renders the pellet model duly sensitive to interaction forces from the cladding.

(iii) The total radial crack volume is now evenly distributed circumferentially. This insures better accuracy in the average stress/strain values, at the cost of insignificant local detail.

(iv) Elastic moduli and other materials properties are now functions of temperature and other operational parameters.

(v) The fundamental mode of calculation has been changed: WAFER-1 calculates time step increments of all system variables, to be added to base values from the preceding time point. WAFER-2 does an absolute base value calculation at each time point for all non-integrator variables. This change saves storage and reduces error accumulation.

(vi) A series of new capabilities has been added to the code: Densification, gaseous swelling and fission gas release.

(vii) The treatment of primary creep and yielding of the cladding has been improved.

The WAFER-2 pellet submodel. — Most of the novel features are introduced through a new finite difference pellet submodel, discussed below: UO_2 pellets crack extensively under irradiation. Further, hour-glassing and clad ridging are real phenomena. Hour-glassing may in some cases be explained from a purely elastic model. Since transversal cracks counteract elastic hour-glassing, we must in those cases conclude that transversal cracks are suppressed by axial forces. The WAFER-2 pellet model allows several transversal cracks to form in the pellet. Before pellet-clad interaction starts, the model therefore predicts little hour-glassing. Power increases beyond the point of incipient interaction cause increased hour-glassing and clad ridging as the axial forces develop. When the cracks are fully closed, the pellet model will behave like an elastic model. The onset of interaction is determined from a simple criterion of stochastic locking between the pellet stack and the cladding. Presently, this criterion is based on calculated hot gap.

The over-all model. — The various improvements of WAFER-2 have significantly reduced storage requirements and running time. Further, reliability of results and code numerical performance have been greatly enhanced. Under a special option the detailed pellet model may be replaced by a one-dimensional model. Thereby the code degenerates into a very efficient one-dimensional code.

Conclusive remarks. — WAFER-2 analyses complete power histories of LWR fuel pins. Normally, a scanning run is executed using the one-dimensional option. Then, selected time intervals, e.g. ramps, are rerun using the full model capability. This cost-saving technique has proven very successful in obtaining complete, detailed analyses for evaluation and planning of experiments and for use in fuel design. The WAFER-2 code is unique by combining state-of-the-art, one-dimensional modelling with detailed ridging analyses in one self-consistent code.

* Work performed under contract with Metallurgy Department, Research Establishment Risø, DK-4000 Roskilde, Denmark.

1. Introduction

The WAFER code is a performance analysis tool for light water reactor fuel pins. It aims at a detailed description of the thermo-mechanical response of the UO_2-pellet/zircaloy--clad system to the entire life-time operating history of the pin. It is designed to compute the local stresses and strains over circumferential clad ridges resulting from pellet-clad mechanical interaction.

The first version, WAFER-1, of the WAFER code has previously been published [1,2].

The version, WAFER-2, to be discussed in this paper features a number of significant improvements relative to WAFER-1, designed to increase reliability and accuracy and decrease storage requirements and processing time:

(i) The pellet crack-pattern calculation has been changed so as to remove arbitrary constraints on crack penetration. This modification implies that more realistic stress--distributions and, consequently, more reliable creep-rates are obtained in the fuel.

(ii) The fact that pellet hourglassing is strongly dependent on the axial interactive forces between fuel column and cladding tube, has been explicitly recognized in the modelling of the pellet, in particular by allowing a large number of transversal cracks. The relationship between pellet hourglassing and clad ridging is established by use of an energy principle that minimizes the total stored deformation energy in the fuel-clad axial interaction system.

(iii) The treatment of radial pellet cracks has been altered so as to include a large number of evenly distributed cracks around the perifery. This improves the accuracy of the average stress/strain calculation of the pellet.

(iv) Important materials properties, e.g. elastic moduli, Poisson's ratios, temperature expansion coefficients, etc., have been made functions of temperature and other operational variables.

(v) The numerical organization of the code has been changed so that it no longer calculates time-step increments of the non-integrator system variables, but rather performs an absolute calculation at each point in time. The use of this method greatly enhances the efficiency of the code and reduces the storage requirements.

(vi) The effects of in-pile densification, gaseous swelling and fission gas release have been included. Five different gas release models from the literature are available on an optional basis.

(vii) Improved models for primary creep and clad yielding have been included. Several models from the literature may be selected, optionally.

The WAFER-2 code offers a multidimensional analysis of a segment of a fuel pin throughout its power history. The pellet hourglassing/clad ridging calculation is automatically activated whenever pellet-clad machanical interaction occurs. Otherwise the code runs as a one-dimensional code. Because of this feature the code is able to do a complete power history analysis, performing ridge calculations as applicable, in a very economic way. The ridge calculation may also be suppressed by input option over selected portions of the power history, so that the code may be operated as a one-dimensional, state-of-the-art fuel performance code at correspondingly reduced costs.

In the following the various submodels of WAFER-2 are explained, emphasizing the new features.

2. The Basic Pellet Model

The basic pellet model used in WAFER-2 offers a structural analysis of a cross-section of a fuel pin. The finite-difference method is used to satisfy the balance equation applicable in each of a number of selected meshpoints along a radius.

Transversal cracking (in planes perpendicular to the axis) is simulated by putting the axial stress equal to minus the plenum pressure. Radial cracking (in planes containing the axis), correspondingly, is simulated by putting the hoop stress equal to minus the plenum pressure. By this method four different versions of the balance equation are to be considered, corresponding to:

(i) the uncracked condition,

(ii) the transversally cracked condition,

(iii) the radially cracked condition, and

(iv) the transversally and radially cracked condition.

Which equation to use in each individual meshpoint depends on the stresses calculated, i.e. an iterative procedure is called for.

A brief derivation of the four versions of the balance equation is given below. The nomenclature is explained in the list at the end of the paper.

The balance equation in axisymmetric geometry in all cases reads:

$$\frac{\sigma_r-\sigma_\theta}{r} + \frac{\partial\sigma_r}{\partial r} = 0 \tag{1}$$

The stresses are given by:

$$\sigma_a = A\{(1-\nu)\varepsilon_a+\nu(\varepsilon_r+\varepsilon_\theta)-(1+\nu)\alpha T-(1-2\nu)\varepsilon_{ao}\} \tag{2}$$

$$\sigma_r = A\{(1-\nu)\varepsilon_r+\nu(\varepsilon_a+\varepsilon_\theta)-(1+\nu)\alpha T-(1-2\nu)\varepsilon_{ro}\} \tag{3}$$

$$\sigma_\theta = A\{(1-\nu)\varepsilon_\theta+\nu(\varepsilon_a+\varepsilon_r)-(1+\nu)\alpha T-(1-2\nu)\varepsilon_{\theta o}\} \tag{4}$$

For the uncracked case the strains are given by:

$$\varepsilon_r = \frac{\partial u}{\partial r} \tag{5}$$

$$\varepsilon_a = \frac{\partial w}{\partial z} = \text{a constant (plane strain)} \tag{6}$$

$$\varepsilon_\theta = \frac{u}{r} \tag{7}$$

In case of transversal cracking we must put $\sigma_a = -p_1$, i.e.

$$\varepsilon_a = \frac{\partial w}{\partial z} = \frac{1+\nu}{1-\nu}\alpha T + \frac{1-2\nu}{1-\nu}\varepsilon_{ao} - \frac{\nu}{1-\nu}\left(\frac{\partial u}{\partial r} + \varepsilon_\theta\right) - \frac{p_1}{A\,(1-\nu)} \tag{8}$$

In case of radial cracking we must put $\sigma_r = -p_1$, i.e.

$$\varepsilon_\theta = \frac{1+\nu}{1-\nu}\alpha T + \frac{1-2\nu}{1-\nu}\varepsilon_{\theta o} - \frac{\nu}{1-\nu}\left(\frac{\partial u}{\partial r} + \frac{\partial w}{\partial z}\right) - \frac{P_1}{A(1-\nu)} \tag{9}$$

The balance equation (1), by use of eqs. (2) through (9), transforms into the four versions:

(i) Uncracked case:

$$(1-\nu)\frac{\partial^2 u}{\partial r^2} + \frac{1-\nu}{r}\frac{\partial u}{\partial r} - \frac{1-\nu}{r^2}u - (1+\nu)\frac{\partial}{\partial r}(\alpha T) - (1-2\nu)\left(\frac{2\varepsilon_{ro}+\varepsilon_{ao}}{r} + \frac{\partial \varepsilon_{ro}}{\partial r}\right) = 0 \tag{10}$$

(ii) Transversally cracked case:

$$\frac{\partial^2 u}{\partial r^2} + \frac{1}{r}\frac{\partial u}{\partial r} - \frac{u}{r^2} - (1+\nu)\frac{\partial}{\partial r}(\alpha T) - (1-\nu)\left(\frac{2\varepsilon_{ro}+\varepsilon_{ao}}{r} + \frac{\partial \varepsilon_{ro}}{\partial r}\right) + \nu\frac{\partial \varepsilon_{ao}}{\partial r} = 0 \tag{11}$$

(iii) Radially cracked case:

$$\frac{\partial^2 u}{\partial r^2} + \frac{1}{r}\frac{\partial u}{\partial r} + \frac{\nu}{r}\frac{\partial w}{\partial z} - \frac{1+\nu}{r}\alpha T - (1+\nu)\frac{\partial}{\partial r}(\alpha T) + \frac{1}{r}\frac{P_1}{A}$$

$$-\left(\frac{\nu}{r}\varepsilon_{ao} + \frac{\varepsilon_{ro}}{r} + \nu\frac{\partial \varepsilon_{ao}}{\partial r} + \frac{\partial \varepsilon_{ro}}{\partial r}\right) = 0 \tag{12}$$

(iv) Transversally and radially cracked case:

$$\frac{\partial^2 u}{\partial r^2} + \frac{1}{r}\frac{\partial u}{\partial r} - \frac{1}{r}\alpha T - \frac{\partial}{\partial r}(\alpha T) - \left(\frac{\varepsilon_{ro}}{r} + \frac{\partial}{\partial r}\varepsilon_{ro}\right) + \frac{1}{r}\frac{P_1}{A(1+\nu)} = 0 \tag{13}$$

Fig. 1 shows a fuel fragment of infinitesimal volume, cut out around a radius, having an angle $d\theta$ and a height dz. It illustrates the increased radial expansion caused by the cracking.

The radial cracks penetrate to radius r', the transversal cracks to radius r". Hereby, three zones are established corresponding to different cracking cases as indicated in the figure.

As a criterion for transversal or radial cracking the model uses a tensile stress limit, called the fracture strength. This limit depends on temperature and other parameters and thus allows the introduction of the effect of crack healing by hot-pressing.

3. The Basic Clad Model

The basic clad model is a one-dimensional finite-difference model. It corresponds closely to the basic pellet model for the uncracked case.

4. The Three-Dimensional Pellet Model

In the three-dimensional context the pellet is conceived as a pile of discs of small thickness. Fig. 2 illustrates this concept. The planes that separate the discs are the potential transversal cracking planes. Within each disc radial cracks may develop as in the basic pellet model.

As axial forces develop in this system, it will be compressed. Further, depending on the radial distribution of these axial forces at the axial location of each individual disc, the potential cracking planes may be tilted relative to each other so that the pile of discs will sway outwards at the pellet top, thus rendering the pellet hourglass-shaped, while the transversal cracks tend to close.

The pellet shape calculated from this model is very sensitive to both magnitude and distribution of axial forces.

In the mathematical implementation of the model each disc is treated in precisely the same way, i.e. only one disc calculation is made. The basic pellet model is used for this purpose. By this simplification it is not possible to account directly for the shift in the radial distribution of the axial forces as a function of axial location. This, however, is not too important as long as the pellet shape may be reasonably correctly defined. The pellet shape is defined by the incremental tilting angle of the end face of the disc. Since all the discs have the same tilting angle, the over-all sway of the pile of discs is derived directly from the incremental tilting angle.

In order to introduce this quantity into the calculation, the condition of plane strain (eq. (6)) is modified as follows:

$$\varepsilon_a = \frac{\partial w}{\partial z} = \text{a constant} - \beta\ (i-1), \tag{14}$$

where β is the incremental tilting angle and i is the radial meshpoint number.

So far the amount of hourglassing is arbitrarily defined by the value of β. If there is no fuel-clad interaction, it is assumed that β is zero, i.e. no hourglassing is calculated. As axial forces due to fuel-clad interaction develop, the value of β is determined from an energy principle, as described in the next section.

For the pellet hourglassing to develop according to the model it is of course necessary to assume that a suitable dish volume is available at the pellet top, either as-fabricated or formed in-pile. Otherwise the hourglassing would be suppressed by the axial forces concentrating on the center region of the end face. The presence of the dish, in turn, implies that the disc elements close to the pellet end have radial distributions of axial force different from those applicable to the elements close to the pellet mid-plane. The use of the energy principle, however, effectively removes the necessity of knowing the precise radial distributions of the axial forces.

5. The Clad Ridging Model

The clad ridging model is based on the concepts of pellet hour-glassing developed in the previous section. The analysis is initiated on the start of fuel-clad interaction.

In WAFER-2 interaction starts when the calculated hot gap at the cross-section considered becomes smaller than an input quantity, specified as a function of time. By this token the model assumes that the relative movement between fuel column and cladding tube is brought to a stop because the fuel at some location above the cross-section considered locks firmly with the cladding, possibly due to random relocation of loose fuel fragments.

For a given degree of pellet hourglassing (choice of tilting angle) a certain amount of ridging will be imposed on the cladding. The ridge shape and the associated axial distri-

butions of stress and strain are established from a shell theory analysis.

An energy minimization principle is used to determine what the correct tilting angle should be.

The basic element in this consideration is the observation that the energy required to form an elasto-plastic ridge of a given magnitude must come from a reduction of stored deformation energy elsewhere in the axial fuel-clad mechanical interaction system. This reduction is obtained largely by a reduction in effective pellet height.

For a dished pellet the effective pellet height is measured at the edge of the dish. Therefore, as the transversal cracks are compressed by axial interaction the effective pellet height diminishes. This causes a reduction in axial interactive force and, hence, in stored deformation energy. In this process the maximum pellet hourglassing that is theoretically obtainable is determined by the dish volume.

For a flat-ended pellet the effective pellet height is measured at the radial location at which the temperature equals the plasticity temperature. The maximum obtainable hourglassing is determined by any dish volume formed during in-pile operation. If no in-pile dishing has occurred, no ridge formation is possible, according to the model.

The model currently calculates the in-pile dish volume. Generally, this quantity is sufficiently large to permit ridging for flat-ended pellets, comparable in size to those obtained for dished pellets.

The compression of the pellet transversal cracks presumes, naturally, that radial cracks are formed to permit fuel fragments at the pellet top to move radially outwards. In this way an internal volume is gradually formed which may to some extent act as a supplement to the dish volume, thus enhancing the possible hourglassing for flat-ended pellets.

Figs. 3(a) and (b) explain these concepts.

Let point A indicate the radial mesh point at which the effective pellet height is measured. For dished pellets this would be the edge of the dish, for flat-ended pellets it would be the point at which the fuel temperature equals the plasticity temperature. On tilting of the stack of fragments the effective height will decrease, provided A is located sufficiently close to the pellet surface. Otherwise it may increase. The hatched area in fig. 3(b) represents the necessary dish volume that must be present for the shown amount of tilting to be possible. When the necessary dish volume equals the actual dish volume, maximum tilting has been obtained.

If the effective pellet height decreases as a function of increasing tilting angle, the axial fuel-clad interaction force is reduced. The total deformation energy stored in the pellet or in the clad per unit length may be calculated from the formula:

$$E = \sum_{\substack{i=1,M \\ k=1,3}} \tfrac{1}{2}\, \sigma_{ki}\, (\varepsilon_{ki} - \alpha_i T_i)\, dA_i/dr \qquad (15)$$

where σ_{ki} and ε_{ki} denote principal stress and strain at i'th meshpoint, α linear heat expansion coefficient, T temperature, dA area increment, dr radial mesh size and M number of meshpoints.

As the tilting angle is increased, the curved pellet shape will impose on the clad to form a circumferential ridge. For a given ridge height (corresponding to a given tilting

angle) the energy stored per unit length in clad ridges is given by:

$$E_r = \sum_{i=1,10} \tfrac{1}{2}\, \sigma_{ti}\, \varepsilon_{ti}\; 2\pi r \cdot t \qquad (16)$$

where σ_t and ε_t denote increments of hoop stress and strain due to ridge formation, r clad mean radius and t clad wall thickness.

Eq. (16) corresponds to a shell theory description of the clad in the axial direction, with stresses and strains recorded in 10 axial points distributed over a half-pellet.

The ridge model is executed by increasing the tilting angle from zero, using increasing steps. For each value of tilting angle a complete disc model calculation is performed, the ridge height is derived from the tilting angle, and an elasto-plastic shell theory analysis of the axially distributed ridge is performed. The stored deformation energies of pellet, clad (not considering the ridge) and ridge are calculated using eqs. (15) and (16). When the sum of these three contributions displays a minimum the tilting angle corresponding to that minimum is calculated and the analysis is finalized for that angle.

Fig. 4 shows a plot of the three energy contributions as well as their sum as a function of tilting angle. The plot uses values from an actual sample case. The minimum displayed by the sum curve is rather well defined because of the significant curvature of the constituant curves.

The energy to be minimized is built up on going from the heat load threshold of pellet--clad mechanical interaction to the heat-load to be considered. If the heat load is temporarily lowered and then raised again, a new interaction threshold is established in dependency of the available hot gap.

If an increase in average permanent clad strain takes place during the approach to the heat-load to be considered, an "ironing" effect on any previously formed ridges results. If the increment in average hoop strain exceeds the previously calculated diametral ridge height divided by the clad diameter, the previous ridge is smoothed out. If previous ridging prevails, it may or may not be increased depending on the heat-load considered, irradiation and strain-hardening condition of the cladding, heat-load threshold of pellet-clad mechanical interaction, and amount of transversal crack and dishing volume available.

The deformation energy available for ridging will be larger for larger dish radius (in case of dished pellets), for larger radius of plastic fuel zone (in case of flat-ended pellets), and for larger pellet length to diameter ratio.

The ridge calculation as explained here requires repetition of the complete disc calculation a number of times, depending on the magnitude of the ridge. Assuming that, on an average, five passes are required, the cost of a ridge calculation is about five times that of the standard disc calculation at that time step. For normal irradiation histories, pellet-clad mechanical interaction occurs only during limited time-intervals. If there is no interaction, the ridge calculation is not attempted. Thus, the cost increase to do the ridge calculation as applicable throughout a normal run will typically be limited within a factor of, say, two.

6. The Creep and Yielding Submodels

WAFER-2 accounts for secondary creep of the fuel, primary and secondary creep of the

cladding and yielding of the cladding.

For temperatures higher than a specified limit fuel creep rates become so high that the material behaves essentially plastically. Therefore, in this region the integration of the fuel creep equations is abandoned and the available strains distributed so as to equalize the principal stresses (hydrostatic condition). This method is much more efficient and gives about the same results.

In the treatment of primary creep in the cladding a method of strain-hardening is applied.

Clad yielding is also treated by a method of strain-hardening. The yield curve is assumed to be linear beyond the yield point, corresponding to a specified slope. The linearity assumption is applicable so long as the generalized strain is limited within a few percent.

Several literature expressions for the various creep-rates are embedded in the code, to be selected through an input indicator.

7. The Densification, Swelling and Fission Gas Release Submodels

Densification is treated by permitting the relative density to vary from the as-fabricated value, to an input value, referred to as the stable density. This variation takes place as follows:

$$D = D_s + (D_o - D_s)e^{-BU/500} \qquad (17)$$

where D is density, BU burnup in MWd/tUO_2 and indices o and s refer to as-fabricated and stable values, respectively.

Swelling is accounted for by two terms, solid swelling and gaseous swelling.

Solid swelling amounts to a fixed percentage per unit of burnup, gaseous swelling is calculated by a model similar to that of Collins et.al. [3].

The swelling contributions, however, are fully effective only after the initial porosity has absorbed a certain amount of fission products.

The fission gas release fraction for each timestep is calculated from a simple model in dependency of temperature, burn-up and time.

The actual release during any time-step is the sum of the release calculated by applying the present release fraction to the gas generated during the present time-step, and the releases calculated by updating the release fractions of all previous time-steps from their latest level to the level of the present release fraction.

One of five different release models from the literature may be selected through input option.

8. The Temperature Submodel

The radial temperature profile is calculated by means of a finite-difference routine utilizing literature expressions for UO_2 and zircaloy thermal conductivities.

The cladding surface temperature is determined from the coolant pressure under the assumption that the coolant temperature is close to saturation. The coolant temperature deviation from saturation may be specified through the input. The clad-coolant heat conductance is determined from the Jens-Lottes formula [4].

The fuel-clad gap conductance is determined from the Ross and Stoute model [5] as modified according to Kjærheim and Rolstad [6]. The influence of the fission gas concentration in the gap is accounted for according to reference [7].

9. Over-All Design of WAFER-2

WAFER-2 has been designed for efficient, reliable and comprehensive fuel performance analyses on a routine basis. It combines the ability of calculating local stress/strain distributions around a circumferential clad ridge with fast and reliable state-of-the-art performance analysis of the parts of the power history during which no pellet-clad mechanical interaction occurs. The code automatically engages the ridge calculation whenever it applies.

To suit the purpose of performing fast analyses of entire power histories without spending computer costs on local detail, the code has been so designed that the ridge calculation may be suppressed through a special input option.

For even faster (and less accurate) analyses, also the axial interaction force calculation may be suppressed through an input option.

The code is equipped with a restart option. At the beginning of each time-step intermediate results may be written to a data storage device. If the processing time exceeds a specified limit the run is orderly terminated and may be restarted from the data file. On restarting, input specification is not necessary but permitted, i.e. adjustment of parameters is possible.

10. Experience with WAFER-2

WAFER-2 has been tested on several experimental cases from the Danish test fuel irradiation program in the DR3 reactor and from the OECD Halden Reactor Project in Norway.

The experience with the code has been very encouraging. For a typical case, i.e. one in which most of the irradiation period elapses without pellet-clad mechanical interaction, while interaction does occur occasionally during relatively short intervals, the running time is reduced by a factor of 5-10, relative to WAFER-1. At the same time reliability and accuracy has been increased.

As an example, the case reported in reference [8], which was originally analyzed by WAFER-1, was rerun with WAFER-2. The running time was 7.5 times shorter and the final ridge height was predicted at 3 microns, diametrically, i.e. accurately within 10 microns, diametrically.

Further, two cases of short-term irradiation in DR3 were simulated by WAFER-2 and resulted in very close agreement between calculated and measured ridge-heights. One pin had flat-ended pellets, the other pin had dished pellets. The results were as follows:

	W/cm	Diametral ridge-height	
		Measured	WAFER-2
Pin 1 (flat-ended)	500	22 μ	24 μ
Pin 2 (dished)	650	25 μ	22 μ

11. Conclusion

The new version, WAFER-2, of the Danish WAFER code constitutes a fast, reliable and

accurate tool for LWR fuel performance analysis. It combines state-of-the-art fuel performance modelling technique with a novel approach to the calculation of the local stress/strain distributions in an elasto-plastic ridge. Comparison of WAFER-2 analyses with results from irradiation experiments has been very successful.

Nomenclature

Symbols:

σ	Stress
r	Radial coordinate
A	$E/(1+\nu)/(1-2\nu)$
E	Elastic modulus
ν	Poisson's ratio
α	Linear heat expansion coefficient
T	Temperature
ε	Strain
w	Axial deflection
u	Radial deflection
z	Axial coordinate
p_1	Plenum pressure

Indices:

a	Axial direction
r	Radial direction
θ	Angular direction
o	Used with strains to indicate plastic strain

References

[1] N.Kjær-Pedersen: "Experience with the Three-Dimensional Fuel Performance Model WAFER". 3rd SMiRT Conf., London, UK, Sept. 1975, Paper D 1/4.

[2] N.Kjær-Pedersen: "Mathematical Description of WAFER-1, A Three-Dimensional Code for LWR Fuel Performance Analysis", Nuc.Eng. and Des. 35 (1975), 387-398.

[3] D.A.Collins, et.al.: "UO_2-Fuel Performance Modelling and Predictive Methods", BNES Conf. on Nuclear Fuel Performance, London, UK, Oct. 1973, Paper 49.

[4] W.H.Jens and P.A.Lottes: "Analysis of Heat Transfer Burn-Out, Pressure-Drop and Density Data for High-Pressure Water", ANL-4627 (1951).

[5] A.M.Ross and R.L.Stoute: "Heat Transfer Coefficient between UO_2 and Zircoloy-2", AECL-1552 (1962).

[6] G.Kjærheim and E.Rolstad: "In-pile Determination of UO_2-Thermal Conductivity, Density Effects and Gap Conductance", HPR-80 (1967).

[7] Combustion Engineering: "Fuel Evaluation Model", CENPD-139-A (1974).

[8] P. Knudsen and N.Kjær-Pedersen: "Performance Analysis of PWR Power Ramp Tests", ASME 75-WA/HT-68 (1975).

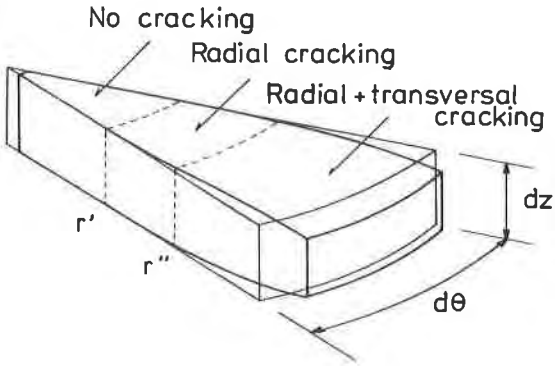

Fig. 1: Basic Pellet Model.

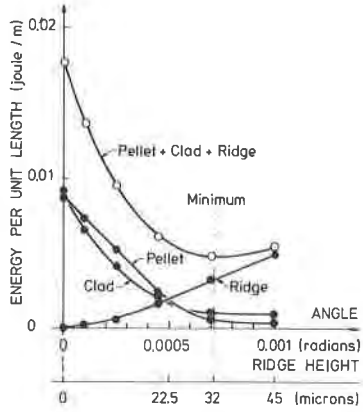

Fig. 4: Energy Minimization Principle.

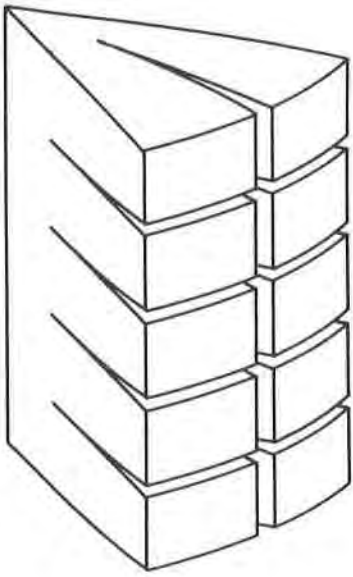

Fig. 2: Multicracked Pellet.

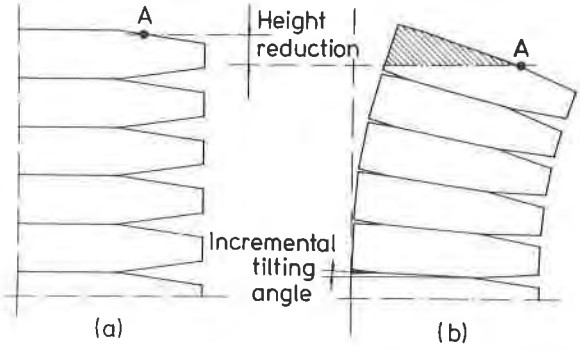

Fig. 3: Pellet Hourglassing and Transversal Crack Closure.